X-ray Diffraction and Electron Paramagnetic Resonance Investigations of the Fluorite Material $Y_{0.25}Ti_{0.15}Zr_{0.6}O_{2-x}$

F. Tietz,* W. Jungen, and P. Lersch

Forschungszentrum Jülich, Institute for Materials and Processes in Energy Systems (IWV-1), D-52425 Jülich, Germany

M. Figaj and K. D. Becker

Institute of Physical and Theoretical Chemistry, Technical University of Braunschweig, Hans-Sommer-Strasse 10, D-38106 Braunschweig, Germany

D. Skarmoutsos

University of Patras, Department of Chemical Engineering GR-26500 Patras, Greece

Received October 11, 2001. Revised Manuscript Received March 7, 2002

The compound $Y_{0.25}Ti_{0.15}Zr_{0.6}O_{2-x}$, to be used as an anode material in solid oxide fuel cells, was synthesized by coprecipitation. X-ray diffraction after sintering at different temperatures revealed no single-phase material up to 1500 °C but indicated two fluorites with different lattice parameters. The inhomogeneity of the material arose from a cation demixing process around 1100−1200 °C, leading to an intermediate fraction of a pyrochlore phase. After reduction in Ar/4% H_2 at 1000 °C, a small decrease (about 0.1%) in the lattice parameter was observed. The electron paramagnetic resonance measurements on reduced samples showed the occurrence of Ti^{3+} ions in at least two sites. Possible reasons for the decrease of the lattice parameter after reduction are discussed.

1. Introduction

During recent years, mixed ionic−electronic conducting oxide ceramics such as perovskites,[1,2] pyrochlores,[3] and fluorites[4] have been considered as improved anode materials in solid oxide fuel cells. The mixed conduction in titanium-containing fluorites was initially investigated back in the late 1980s.[5,6] Recently, the stability region of the fluorite phase in the Y−Zr−Ti−O system was established at 1500 °C, and it was revealed that up to 18 mol % Ti can be incorporated into the fluorite structure with the single-phase cubic nature of the material being maintained.[7] The material investigated in this study, $Y_{0.25}Ti_{0.15}Zr_{0.6}O_{2-x}$, is a limiting composition toward a two-phase region[7] and was previously characterized by dilatometry.[8] The thermal expansion coefficient between room temperature and 1000 °C of this compound is 10.7×10^{-6} K^{-1}, the same value as for 8 mol % yttria-stabilized zirconia (YSZ), the widely used electrolyte material in solid oxide fuel cells. However, an abnormal length change was observed when the material was exposed to reducing atmospheres, as shown in Figure 1.

The small decrease in length is very intriguing because materials containing multivalent cations that are able to be reduced in atmospheres with low oxygen partial pressures such as lanthanum chromites ($Cr^{4+} \rightarrow Cr^{3+}$)[2,9,10] and ceria materials ($Ce^{4+} \rightarrow Ce^{3+}$)[8,11] usually tend to expand during reduction. This is mainly due to the larger ionic radius of the cation in the lower valence state but also, to some extent, to the release of oxygen from the lattice and the electrostatic repulsion of the neighboring cations at the oxygen vacancy formed. Therefore, it was expected that $Y_{0.25}Ti_{0.15}Zr_{0.6}O_{2-x}$ would also expand through the formation of Ti^{3+} ions rather than undergoing a small shrinkage. Also, the shape of the transition looks rather unusual because the above-mentioned process of cation reduction and oxygen release is diffusion-limited and a diffusion coefficient

* To whom correspondence should be addressed: Dr. F. Tietz, Forschungszentrum Jülich, Institute for Materials and Processes in Energy Systems (IWV-1), D-52425 Jülich, Germany. Tel.: +49/2461/615007. Fax: +49/2461/612455. e-mail: f.tietz@fz-juelich.de.

(1) Fagg, D. P.; Kharton, V. V.; Kovslevsky, A. V.; Viskup, A. P.; Naumovich, E. N.; Frade, J. R. *J. Eur. Ceram. Soc.* **2001**, *21*, 1831.

(2) Pudmich, G.; Boukamp, B. A.; Gonzalez-Cuenca, M.; Jungen, W.; Zipprich, W.; Tietz, F. *Solid State Ionics* **2000**, *135*, 433.

(3) Holtappels, P. P.; Poulsen, F. W.; Mogensen, M. *Solid State Ionics* **2000**, *135*, 675.

(4) Kaiser, A.; Feighery, A. J.; Irvine, J. T. S. Novel Highly Titania Doped YSZ Anodes for SOFCs. In *Proceedings of the 6th International Symposium on Solid Oxide Fuel Cells (SOFC−VI)*; Singhal, S. C., Dokiya, M., Eds.; The Electrochemical Society: Pennington, NJ, 1999; p 541.

(5) Liou, S. S.; Worrell, W. L. *Appl. Phys. A* **1989**, *49*, 25.

(6) Kopp, A.; Näfe, H.; Weppner, W.; Kontouros, P.; Schubert, H. Ionic and Electronic Conductivity of TiO_2−Y_2O_3-Stabilized Tetragonal Zirconia Polycrystals. In *Proceedings Science and Technology of Zirconia V*; Badwal, S. P. S., Bannister, M. J., Hannink, R. H. J., Eds.; Technomic Publishing Co.: Lancaster, PA, 1993; p 567.

(7) Feighery, A. J.; Irvine, J. T. S.; Fagg, D. P.; Kaiser, A. *J. Solid State Chem.* **1999**, *143*, 273.

(8) Tietz, F. In Peculiarities in the Thermal Expansion Behavior of Ceramic Fuel Cell Materials. *Proceedings of the 9th CIMTEC−World Ceramic Congress and Forum on New Materials*; Vincenzini, P., Ed.; Techna Publishers S.r.l.: Faenza, Italy, 1999; Vol. 24: Innovative Materials in Advanced Energy Technologies, p 61.

(9) Armstrong, T. R.; Stevenson, J. W.; Pederson, L. R.; Raney, P. E. *J. Electrochem. Soc.* **1996**, *143*, 2919.

(10) Larsen, P. H.; Hendriksen, P. V.; Mogensen, M. *J. Therm. Anal.* **1997**, *49*, 1263.

(11) Mogensen G.; Mogensen, M. *Thermochim. Acta* **1993**, *214*, 47.

10.1021/cm011252h CCC: $22.00
Published on Web 04/25/2002

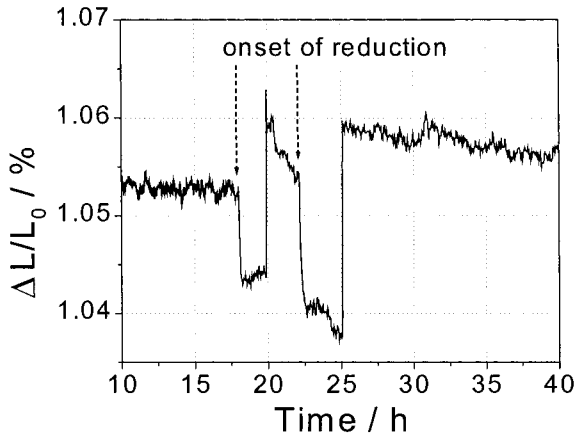

Figure 1. Length change of $Y_{0.25}Ti_{0.15}Zr_{0.6}O_{2-x}$ during isothermal oxidation−reduction cycling at 1000 °C using flowing gases of Ar/20% O_2 and Ar/4% H_2 [corresponding to a change in oxygen partial pressure from $p(O_2) = 0.2$ to $p(O_2) \approx 10^{-18}$ bar).

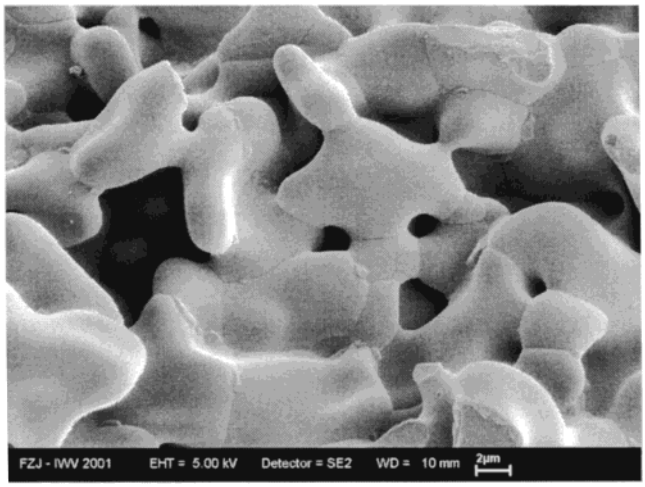

Figure 2. Surface of polycrystalline $Y_{0.25}Ti_{0.15}Zr_{0.6}O_{2-x}$ after sintering at 1500 °C for 5 h. Note the small crystalline segregations along the grain boundaries.

can be deduced from the dimensional change,[11] whereas the transitions from the oxidized to the reduced state and vice versa are very sharp for $Y_{0.25}Ti_{0.15}Zr_{0.6}O_{2-x}$ (Figure 1), indicating a rapid ionic−electronic process. A rough estimation can be made assuming that ionic transport is the rate-limiting step and considering a diffusion coefficient of $D \approx 1 \times 10^{-5}$ cm^2/s at 1000 °C as for YSZ[12] and a porous sintered body with a typical grain size of $d = 2-10$ μm (Figure 2). In this case, the reduction process should be completed after 0.1 s. However, because of larger agglomerates, the process requires 50−100 s for completion according to the experimental results (Figure 1).

Similar results were also reported for titanium-rich perovskites. From ref 9, it was shown that the addition of Ti reduces the swelling of lanthanum chromites, and in ref 2, it was shown that 50% of Ti compensated for the increase in length due to the chromium reduction. However, considering the whole solid solution (e.g., $La_{0.7}Ca_{0.3}Cr_{1-y}Ti_yO_{3-\delta}$) a third unusual fact emerges (Figure 3): although the length changes are compensated at a Cr/Ti ratio of 1:1, the end member $La_{0.7}Ca_{0.3}CrO_{3-\delta}$ shows a swelling that is much larger than the shrinkage of the other end member $La_{0.7}Ca_{0.3}TiO_{3-\delta}$.

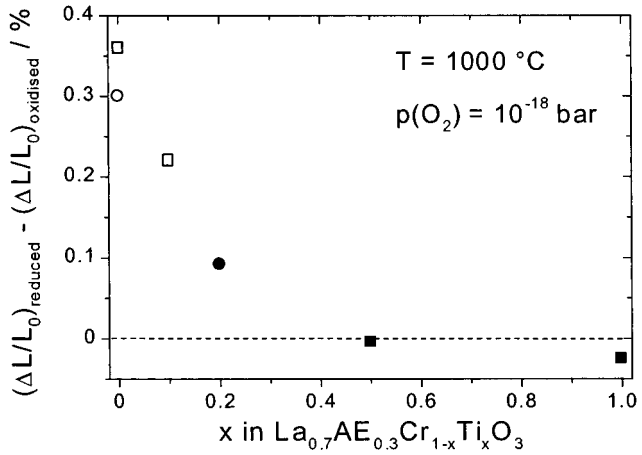

Figure 3. Length changes between $p(O_2) = 0.2$ and $p(O_2) \approx 10^{-18}$ bar at 1000 °C for the perovskite solid solution $La_{0.7}AE_{0.3}Cr_{1-y}Ti_yO_{3-\delta}$ (AE = alkaline-earth element). Circles and squares refer to samples with AE = Sr and AE = Ca, respectively. Open symbols indicate values taken from the literature.[9]

In this study, the compound $Y_{0.25}Ti_{0.15}Zr_{0.6}O_{2-x}$ is investigated in more detail by X-ray diffraction (XRD) and electron paramagnetic resonance (EPR). EPR is widely used to study the defect chemistry of diamagnetic solids (see, e.g., ref 13) and is very sensitive to structural changes of the EPR probe's coordination.[14] Experiments performed in this investigation aim at a better understanding of the phenomenon of dimensional shrinkage of titanium-rich oxide ceramics. A (Ti,Zr)-containing fluorite material was chosen instead of a Ti−Cr perovskite because the chromium signal in EPR measurements might interfere with the titanium signal and because of the better magnetic dilution. Furthermore, EPR investigations of titanium in zirconia materials are available and are considered in the interpretation and discussion of our results.

2. Experimental Section

The $Y_{0.25}Ti_{0.15}Zr_{0.6}O_{2-x}$ powder was prepared by coprecipitation. The starting materials were $Y(NO_3)_3 \cdot xH_2O$ (Chempur), $ZrOCl_2 \cdot 8H_2O$ (Merck), and $TiCl_3$ dissolved in 10 mol % HCl (Merck). To synthesize 500 g of powder, the appropriate amounts of yttrium nitrate and zirconium oxidichloride were dissolved in distilled water, the corresponding amount of $TiCl_3$ solution was added, and the mixture was slowly added to a solution consisting of 500 mL of concentrated ammonium and 2 L of distilled water. During the continuous addition of the salt solution, the aqueous mixture was intensively stirred, and a white precipitate formed. The precipitate was subsequently filtered out and carefully washed with distilled water until no chloride ions could be detected by silver chloride. The precipitate was dried overnight at 120 °C in a drying furnace and calcined at 750 °C. A chemical analysis of the powder was performed using inductively coupled argon plasma with optical atomic emission spectroscopy (ICP−OES) giving a composition of $Y_{0.243\pm0.007}Ti_{0.147\pm0.004}Zr_{0.611\pm0.018}O_{2-x}$, which matches very well with the nominal composition.

(12) Sasaki, K.; Maier, J. *Solid State Ionics* **2000**, *134*, 303.

(13) Pilbrow, J. R. *Transition Ion Electron Paramagnetic Resonance*; Clarendon Press: Oxford, U.K., 1990.

(14) Böttcher, R.; Klimm, C.; Michel, D.; Semmelhack, H.-C.; Völkel, G.; Gläsel, H.-J.; Hartmann, E. *Phys. Rev. B* **2000**, *62*, 2085.

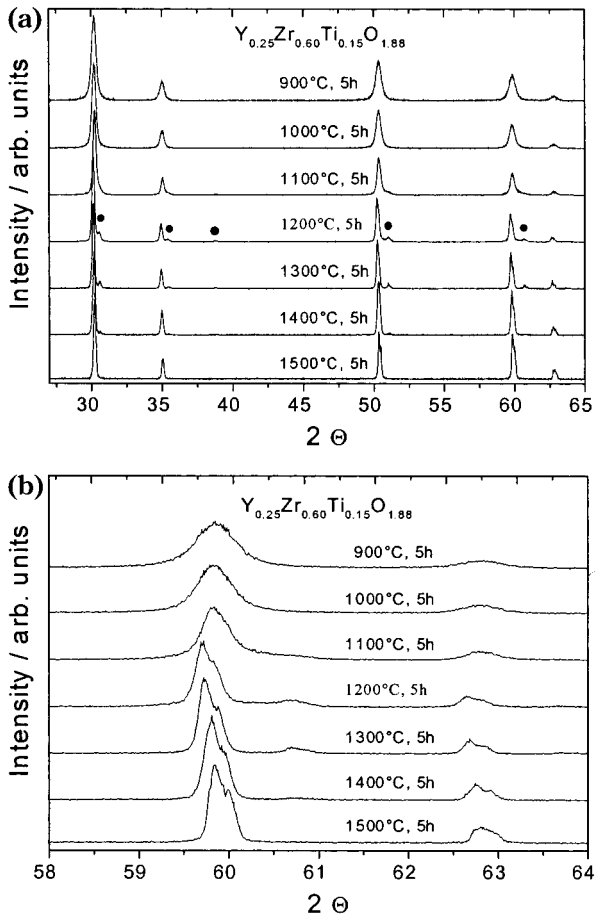

Figure 4. (a) XRD patterns of $Y_{0.25}Ti_{0.15}Zr_{0.6}O_{2-x}$ after sintering in air between 900 and 1500 °C for 5 h at each temperature. Between 1200 and 1400 °C, additional reflections of the pyrochlore structure appear (filled circles). (b) Enlarged XRD patterns of $Y_{0.25}Ti_{0.15}Zr_{0.6}O_{2-x}$ in the 2Θ region from 58 to 64°. The 331 reflection at 2Θ = 59.8° is slightly shifted toward smaller 2Θ values between 1200 and 1400 °C. Also, after sintering at 1500 °C, a doublet remains that is not visible in the overall pattern of Figure 4a but that is significantly broader than can be expected from the intensities of the $K_{\alpha1}$ and $K_{\alpha2}$ radiation of the copper source.

X-ray diffraction measurements were performed at room temperature using a Siemens D5000 diffractometer and Cu Kα radiation.

Recordings of EPR spectra were taken from 108 to 400 K by means of a commercial Bruker EMX spectrometer employing microwave radiation of 9.42 GHz (X-band). The values of *g* factors were measured relative to a diphenylpicrylhydrazil (DPPH) standard. The samples were reduced by annealing in an Ar/5% H_2 environment for 18 h at a temperature of 1000 °C and an oxygen partial pressure, $p(O_2)$, of $10^{-19.3}$ bar. $p(O_2)$ was measured by a zirconia EMF cell. The sample was held in the gas stream during the subsequent cooling.

3. Results and Discussion

(a) XRD. After calcination at 750 °C, small amounts of the powder were subjected to sintering experiments between 900 and 1500 °C to evaluate the phase evolution with increasing temperature.[15] At 900 and 1000 °C, the material is still inhomogeneous and disordered, as can be concluded from the peak broadening in the XRD patterns (Figure 4). With increasing temperature, the reflections become sharper and more intense; therefore, the $K_{\alpha1}/K_{\alpha2}$ spitting becomes evident, e.g., at 2Θ ≈ 60° (Figure 4b). Furthermore, additional reflections start to appear at about 1200 °C (Figure 4a), which can be attributed to the pyrochlore-type structure ["$Y_2(Ti,Zr)_2O_7$"]. The intensity of these additional reflections decreases again with increasing temperature, and at 1500 °C, only the XRD pattern of the fluorite structure appears. This behavior can be explained by the fact that the composition is close to the two-phase region in the phase diagram[7] and that this compound tends to decompose into fluorite and pyrochlore. The appearance of the pyrochlore structure can be regarded as a demixing of cations during sintering in which the fluorite phase is depleted of Y and Ti ions. Considering the small peak heights relative to the fluorite reflections, it is assumed that this phase separation is revealed by the crystalline segregations along the grain boundaries, as shown in Figures 2 and 5. This phase separation is accompanied by the occurrence of a peak shift of the fluorite reflections (Figure 4b) in the temperature region at which the pyrochlore peaks appear. As a result, the cubic lattice parameter *a* of the fluorite phase increases slightly from the sample sintered at 1100 °C to that sintered at 1200 °C (Figure 6). With increasing temperature, the solubilities of Y and Ti increase, and therefore, the lattice parameters after sintering change continuously up to 1400 °C.

By 1500 °C, the pyrochlore peaks completely disappear. The fluorite XRD reflections now are found to be composed of at least two constituents, as can be seen from the different peak profile at 2Θ = 62.8° (Figure 4b). An intensity profile analysis revealed that a fit with two or three sets of $K_{\alpha1}/K_{\alpha2}$ doublets gives a much better agreement with the intensity profiles than a fit with only one doublet. Hence, it can be assumed that the former pyrochlore grains have transformed into fluorite grains because of the better solubilities of Ti and Y in the material and the homogeneity of the sample. From the intensity profile analysis of the XRD pattern at 1500 °C, it was possible to derive two fluorite lattice parameters (Figure 6). This result, however, shows that the sample was not yet properly homogenized after 5 h of sintering, so the two lattice parameters should be

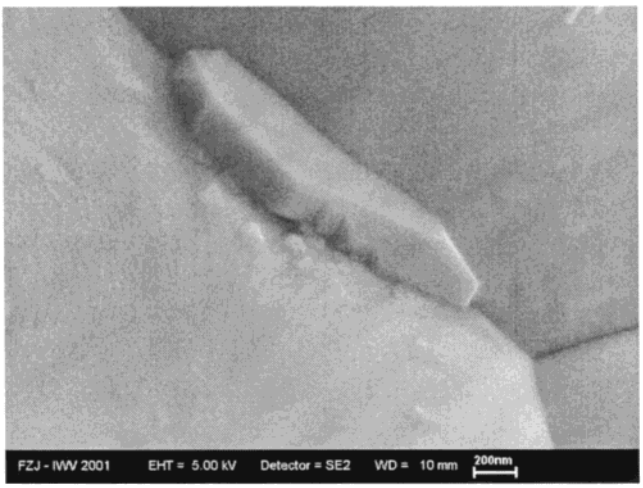

Figure 5. Small crystallite grown along a grain boundary of polycrystalline $Y_{0.25}Ti_{0.15}Zr_{0.6}O_{2-x}$ heat-treated at 1500 °C for 5 h in air.

(15) Tietz, F.; Fischer, W.; Hauber, T.; Mariotto, G. *Solid State Ionics* **1997**, *100*, 289.

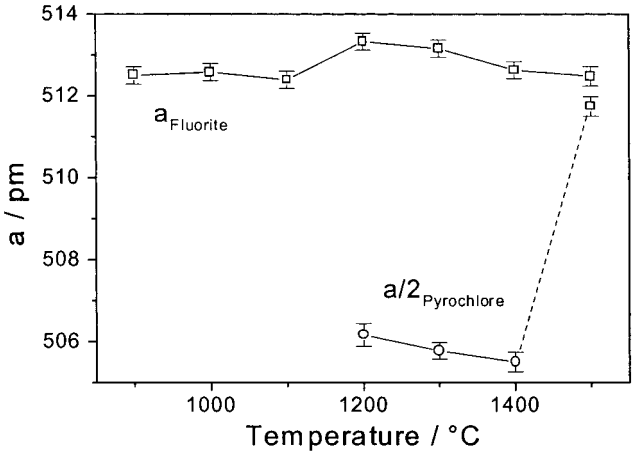

Figure 6. Lattice parameters of the compound $Y_{0.25}Ti_{0.15}Zr_{0.6}O_{2-x}$ after sintering in air between 900 and 1500 °C for 5 h at each temperature. The lattice parameters of the fluorite structure are shown as open squares. Because of the appearance of the pyrochlore structure between 1200 and 1400 °C, these lattice parameters are shown as *a*/2 to indicate the similarity of the two structure types.

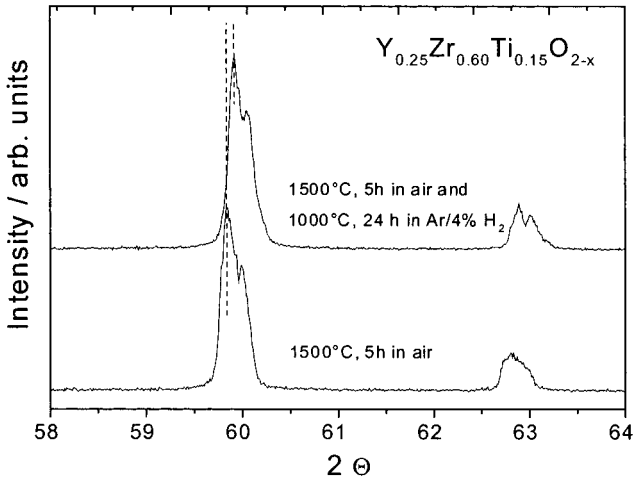

Figure 7. Enlarged XRD patterns of $Y_{0.25}Ti_{0.15}Zr_{0.6}O_{2-x}$ in the 2Θ region from 58 to 64° after sintering at 1500 °C (bottom) and subsequent reduction in Ar/4% H_2 at 1000 °C (top). The 311 peak at 2Θ = 59.8° is slightly shifted toward larger 2Θ values in the case of the reduced sample, as indicated by two dashed lines.

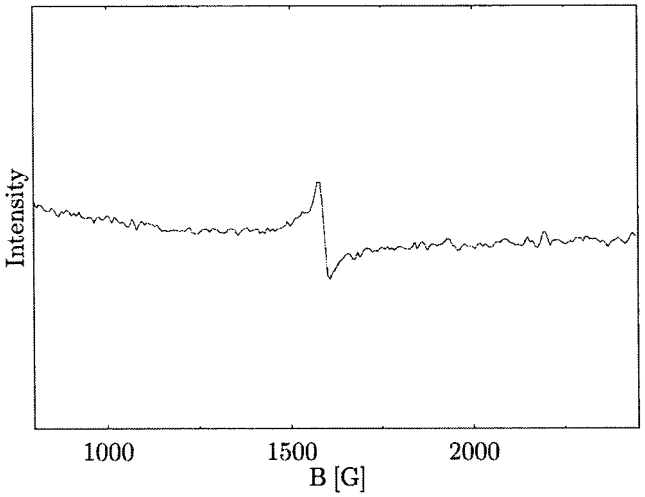

Figure 8. Room-temperature EPR spectrum of oxidized $Y_{0.25}Ti_{0.15}Zr_{0.6}O_{2-x}$. The small signal at low fields is due to Fe^{3+}, which is present as an impurity.

regarded as the most predominant crystal lattice parameters of a bimodal chemical distribution of fluorite grains with high and low amounts of the substituting cations.

Better homogeneity can be expected when the samples are exposed to longer sintering times. Therefore, these results confirm the Y−Zr−Ti−O phase diagram for which the samples were heated for up to 36 h.[7] However, in the present study, the sintering schedules were strongly related to solid oxide fuel cell (SOFC) fabrication steps,[16,17] and no attempt was made to homogenize the material further by applying longer sintering times.

In addition to the investigations of oxidized powder samples, the material sintered at 1500 °C was subsequently heat-treated at 1000 °C for 24 h in Ar/4% H_2. After this reduction step, the dark black sample was again investigated by XRD. As can be seen in Figure 7, the reflections retained their doublet shape but were shifted to higher 2Θ values. For the 311 reflection at about 2Θ = 59.8°, this shift amounts to 0.1°, as shown in Figure 7. Correspondingly, the two lattice parameters of the oxidized sample [$a_{Fluorite1}$ = 512.5(2) pm, $a_{Fluorite2}$ = 511.7(2) pm], which are in good agreement with the value of $a_{Fluorite}$ = 512.09(5) pm reported in ref 18, were shifted by about 0.7 pm to smaller values in the reduced state [$a_{Fluorite1}$ = 511.9(4) pm, $a_{Fluorite2}$ = 511.0(2) pm], corresponding to a change in lattice parameters of about 0.1%. This length change is 5 times larger than the dimensional changes measured by dilatometry (Figure 1). However, a direct conclusion cannot be drawn from this difference because one set of values was measured at room temperature (XRD) and the other values at 1000 °C (dilatometry).

(b) EPR. In the room-temperature spectrum of the oxidized sample sintered at 1500 °C (see Figure 8), only one signal at low field with a *g* factor of *g* = 4.28 could be observed. Such a value is typical of a powder spectrum of a d^5 ion at a site of low symmetry, where the crystal field causes a zero-field splitting of spin states larger than $h\nu$.[13] As no hyperfine splitting is observed, Mn^{2+} (with a natural abundance of 100% of ^{55}Mn, which has a nuclear spin of $^5/_2$ and a typical hyperfine splitting of about 90 G) can be excluded. The most probable candidate is therefore Fe^{3+}. Iron is a common impurity in many metal oxides, and Cr^+ is chemically not favorable in this matrix.

After reduction of the sample, an intense signal at *g* ≈ 1.9 is observed at room temperature. Characteristically, EPR signals of this *g* factor are due to d^1 ions. Color centers should show smaller deviation from the free-electron *g* factor of *g* = 2.0023. Because the signal intensity is too large to be caused by impurities, only Ti^{3+} and Zr^{3+} can be considered as reasonable paramagnetic sources of the signal. We dismiss Zr^{3+} (although several authors report on its existence in reduced stabilized zirconias, e.g., ref 19) and attribute this signal to Ti^{3+} for two reasons: First, Swider and

(16) Simwonis, D.; Thülen, H.; Dias, F. J.; Naoumidis, A.; Stöver, D. *Mater. Process. Technol.* **1999**, *92*−*93*, 107.
(17) Tietz, F.; Dias, F. J.; Dubiel, B.; Penkalla, H. J. *Mater. Sci. Eng.* **1999**, *B68*, 35.
(18) Kaiser, A.; Feighery, A. J.; Fagg, D. P.; Irvine, J. T. S. *Ionics* **1998**, *4*, 215.

Worrell[20] and Merino et al.[21] showed independently that, in reduced Ti-doped stabilized zirconia, an EPR signal with a similar g factor depends linearly on the titanium content of the samples. Second, in the reoxidation kinetics of strongly reduced zirconia, He et al.[22] observed two processes exhibiting different kinetics, with the faster process being the oxidation of Zr^{3+} and the slower process the oxidation of an unknown impurity, most likely Ti^{3+}. Their experiments confirmed the necessity of oxygen partial pressures lower than those that can be attained with gas mixtures to reduce Zr^{4+} to Zr^{3+}. The line shape of this powder signal is neither Lorentzian nor Gaussian, indicating an anisotropic g factor and an enhanced line width. The observation at temperatures as high as 300 K points to Ti^{3+} at sites of low symmetry. This could lead to a splitting of the ground state, leaving an orbital singlet as the lowest state, thus reducing the angular momentum and the spin−lattice coupling and consequently enhancing the relaxation time.[23] The reduction of symmetry can be explained by an adjacent oxygen vacancy or by a Jahn−Teller distortion as is reported for the isoelectronic Sc^{2+} in the fluorite structure.[24] d^1 ions at sites of high symmetry are usually not detected at temperatures far above 77 K.[23] Spectra recorded below a temperature of about 150 K show a drastic change in line shape. This leads to the presumption that the low-temperature spectra is the sum of two signals. The second signal could be due to Ti^{3+} at sites exhibiting a stronger temperature dependence of the relaxation time. Figure 9 shows the temperature dependence of the EPR spectra from 108 to 400 K. The overall signal intensity decreases rapidly, but the line width remains nearly constant.

We tried a deconvolution of the spectra on the assumption that, at high temperatures, only the Ti^{3+} ions exhibiting the longer relaxation time contribute to the observed signal. A calculated axial powder spectrum with $g_\perp = 1.87$, $g_\parallel = 1.97$, $\Delta B_\perp = 130$ G, and $\Delta B_\parallel = 70$ G reproduces the spectrum recorded at 350 K quite well (Figure 10). The differences between the calculated and experimental spectra in the outer regions of the signal can be attributed to the relaxation-time-broadened resonance arising from the presence of Ti^{3+} at the second crystal site. It should be noted that the line widths are too large to differentiate between axial or even lower symmetry, but the axial case is more likely.

Taking the approximate parameters of the axial spectrum at 350 K and fitting the experimental spectrum at 108 K with these parameters (with minor changes in line width), one can calculate a differential spectrum. This differential spectrum can be described as a single-line spectrum with a shape that could well represent an isotropic EPR signal with nearly Lorentzian line shape (Figure 11). This leads to the assumption that the second Ti site with the short relaxation time

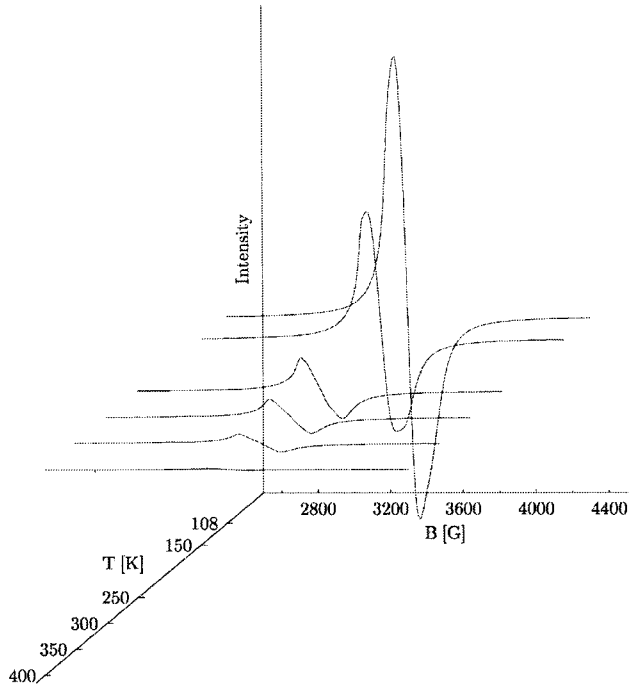

Figure 9. EPR spectra of reduced $Y_{0.25}Ti_{0.15}Zr_{0.6}O_{2-x}$ taken at several temperatures from 108 to 400 K as indicated in the graph.

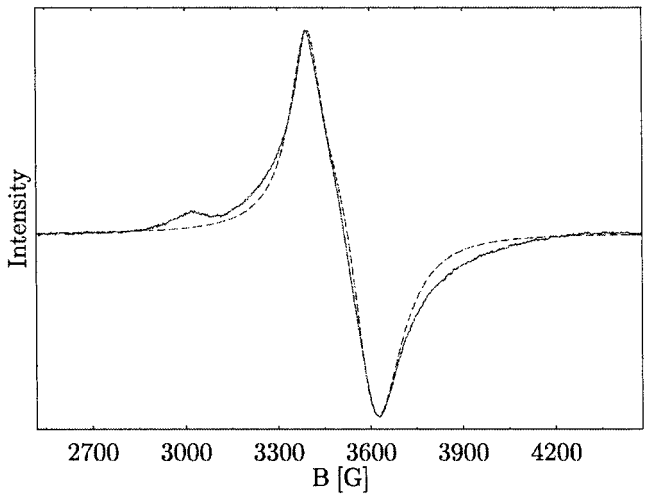

Figure 10. Axial spectrum of reduced $Y_{0.25}Ti_{0.15}Zr_{0.6}O_{2-x}$ at 350 K. The solid line shows the experimental spectrum, and the broken line shows the calculated spectrum. The small feature in the experimental spectrum near $B = 3000$ G is due to a cavity resonance.

at room temperature exhibits a cubic or dynamically averaged symmetry.

In the case of the axial site, the difference between the line widths for the transverse or parallel orientation of the magnetic field with respect to the symmetry axis and the minor dependence of the line width on temperature are typical of a static distribution of the crystal field. The high disorder of the structure containing three kinds of cations and about 6% anion vacancies in the oxidized state can readily explain this distribution.

Swider and Worrell[20] reported an EPR signal at $g \approx 3.73$ in samples with high titanium contents and attributed this signal to antiferromagnetic coupling in $Ti^{3+}-Ti^{3+}$ clusters. A similar signal could not be detected in this work.

(19) Azzoni, C. B.; Paleari, A. *Phys. Rev. B* **1991**, *44*, 6858.
(20) Swider, K. E.; Worrell, W. L. *J. Electrochem. Soc.* **1996**, *143*, 3706.
(21) Merino, R. I.; Orera, V. M.; Lomonova, E. E.; Batygov, S. Kh. *Phys. Rev. B* **1995**, *52*, 6150.
(22) He, T.; Becker, K. D.; Tannhauser, D. S. *Ber. Bunsen-Ges. Phys. Chem.* **1995**, *99*, 658.
(23) Orton, J. W. *Electron Paramagnetic Resonance: An Introduction to Transition Group Ions in Crystals*; Iliffe Books: London, 1968.
(24) Höchli, U. T. *Phys. Rev.* **1967**, *162*, 262.

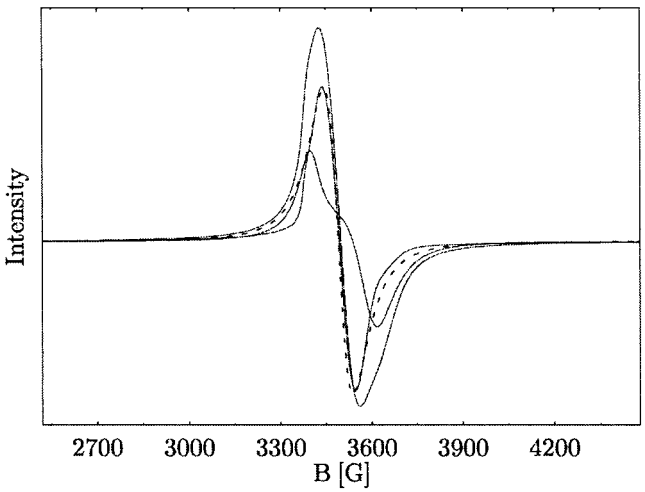

Figure 11. EPR spectrum of reduced $Y_{0.25}Ti_{0.15}Zr_{0.6}O_{2-x}$ at 108 K, extrapolated axial spectrum and differential spectrum (solid lines), and calculated isotropic signal with Lorentzian line shape (dashed line).

Generally, several reasons might be responsible for the observed shrinkage of the samples during oxidation−reduction cycling, either as sintered bodies in dilatometry or as polycrystalline powder in XRD: (a) magnetic interactions as mentioned in ref 20, although no experimental evidence for antiferromagnetic interactions was found in the present ESR study; (b) a dynamic Jahn−Teller effect of the Ti^{3+} ions giving rise to a contraction of the coordination polyhedron around the ions upon reduction; or (c) electronic interactions between Ti^{3+} ions. A possible explanation could be the changing band structure of Ti-containing zirconia.[25] With increasing Ti concentration, the localized Ti 3d states begin to overlap and form a Ti 3d band. The electrons contributing to this band during reduction of the sample can be regarded as delocalized, at least among Ti^{3+} ions that are not more than three Ti−Ti distances away[25] (small polarons), resulting in small attractive forces between these Ti^{3+} ions as a result of the band widening.[26]

4. Conclusions

Sintering experiments in the regime of sintering temperature and dwell time relevant for SOFC fabrication identified two fluorite phases in $Y_{0.25}Ti_{0.15}Zr_{0.6}O_{2-x}$ by XRD, indicating an unsatisfactory inhomogeneity of the powder arising from a cation demixing process around 1100−1200 °C. A two-phase material in the sintering temperature regime relevant to SOFC component fabrication does not make this composition a serious candidate for application as an anode material.

The small decrease in cubic lattice parameters upon reduction confirms the shrinkage of sintered bodies observed previously by dilatometry. The reduction of $Y_{0.25}Ti_{0.15}Zr_{0.6}O_{2-x}$ leads to the formation of Ti^{3+} ions. The ESR spectra provide evidence that these paramagnetic ions are present at two sites: one site with axial symmetry and another with cubic symmetry. The spectra also indicate that there is a distribution of axial sites in the structure, which again reflects an inhomogeneous distribution of cations.

Acknowledgment. The authors thank M. Michulitz and H. Lippert (FZJ−ZCH) for the chemical analysis measurement and E. Wessel (FZJ−IWV-2) for the SEM images. Financial support from the German−Greek bilateral research and technology program (GRI-99/095) is gratefully acknowledged.

CM011252H

(25) Kobayashi, K.; Yamaguchi, S.; Higuchi, T.; Shin, S.; Iguchi, Y. *Solid State Ionics* **2000**, *135*, 643.

(26) Cox, P. A. *The Electronic Structure and Chemistry of Solids*; Oxford Science Publications: Oxford, U.K., 1987.